

The Stau Neutralino Co-annihilation Region at an International Linear Collider

Vadim Khotilovich,[†] Richard Arnowitt,[†] Bhaskar Dutta,^{*} and Teruki Kamon[†]

[†]*Department of Physics, Texas A&M University,
College Station, TX 77807, USA*

^{*}*Department of Physics, University of Regina,
Regina, Saskatchewan S4S 0A2, Canada*

Abstract

We probe the stau-neutralino co-annihilation domain of the parameter space allowed by the current experimental bounds on the light Higgs mass, the $b \rightarrow s\gamma$ decay, and the amount of neutralino cold dark matter within the framework of minimal SUGRA models at a 500 GeV e^+e^- linear collider. The most favorable signals of SUSY are stau pair production and neutralino pair production where the small mass difference between the lighter stau and the lightest neutralino in the co-annihilation region is ~ 5 -15 GeV and hence generates low-energy tau leptons in the final state. This small mass difference would be a striking signal of many SUGRA models. We find that a calorimeter covering down to 1° from the beams is crucial to reduce the two-photon background and the mass difference could be measured at a level of 10% with 500 fb^{-1} of data where an invariant mass of two-tau jets and missing energy is used as a discriminator.

1 Introduction

Since an international electron-positron (e^-e^+) linear collider (ILC) can measure particle masses very accurately, there is a growing consensus that the next high energy machine to be built after the Large Hadron Collider (LHC) should be an ILC. Such a machine is technically feasible and the initial consensus is for the TESLA design [1]. The siting is still under discussion.

There has been in the past a huge amount of analysis on methods of detecting SUSY at an ILC. However, the minimal supergravity (mSUGRA) model [2, 3, 4], has several special aspects that make its predictions clearer and more directly accessible to experimental study. Hence it is worthwhile to examine this particular model. The existing experiments have already begun to restrict the SUSY parameter space significantly. Most significant of these are the amount of cold dark matter (CDM), the Higgs mass bound, the $b \rightarrow s\gamma$ branching ratio, and (possibly) the muon a_μ anomaly.

The allowed parameter space, at present, have three distinct regions [5]: (i) the stau neutralino ($\tilde{\tau}\text{-}\tilde{\chi}_1^0$) co-annihilation region where $\tilde{\chi}_1^0$ is the lightest SUSY particle (LSP), (ii) the $\tilde{\chi}_1^0$ having a larger Higgsino component (focus point) and (iii) the scalar Higgs (A^0, H^0) annihilation funnel ($2M_{\tilde{\chi}_1^0} \simeq M_{A^0, H^0}$). These three regions have been selected out by the CDM constraint. (There stills exists a bulk region where none of these above properties is observed, but this region is now very small due to the existence of other experimental bounds.) The distinction between the above regions can not be observed in the dark matter experiments where only the mass of the lightest SUSY particle would be obtained. However these regions can be observed at the ILC or the LHC where the particles will be produced directly and their masses will be measured.

The three dark matter allowed regions need very precise measurements at the colliders to confirm which is correct. Since the ILC is suitable for making precision measurements, the cosmologically allowed parameter space is under a great deal of scrutiny. In this paper we choose to work with the $\tilde{\tau}\text{-}\tilde{\chi}_1^0$ co-annihilation region. We note that many SUGRA models possess a co-annihilation region and if the a_μ anomaly maintains, it is the only allowed region for mSUGRA. Coannihilation is characterized by a mass difference (ΔM) between $\tilde{\tau}$ and $\tilde{\chi}_1^0$ of about 5-15 GeV. This narrow mass difference allows the $\tilde{\tau}$'s to co-annihilate in the early universe along with the $\tilde{\chi}_1^0$'s in order to produce the current amount of dark matter density of the universe. The co-annihilation region has a large extension for $m_{1/2}$, up to 1-1.5 TeV, and can be explored at the LHC. The main difficulty, however, in probing this region is the small ΔM value. This ΔM needs to be measured very accurately in order to claim that the co-annihilation explains the dark matter content of the universe. However, the small ΔM value generates signals with very low energy tau (τ) leptons and thus makes it difficult to discover this region at any collider due to the large size of the standard model (SM) and SUSY background (BG) events. It is this question for the ILC that we address in this paper.

At an ILC, a major source of the SM backgrounds is the large two-photon events. The previous studies [6, 7] use counting experiments to achieve their results. The discovery significance is calculated using $N_{\text{signal}}/\sqrt{N_{\text{BG}}}$ in Ref. [6], while in Ref. [7], the $\tilde{\tau}_1$ mass is measured using the threshold method where they either scan over various center-of-mass (CM) energies or assume the mass of the LSP is known from the \tilde{e} and the $\tilde{\mu}$ decays (to set the beam energy) in order to achieve the maximum sensitivity for a given $\tilde{\tau}_1$ mass. However, as shown in Sec. 3, we study the scenarios where the \tilde{e} and $\tilde{\mu}$ masses are too heavy to be produced at a 500 GeV machine.

We investigate the accuracy of measuring ΔM by analyzing the shapes of invariant mass distributions of two τ jets and unbalanced event transverse momentum (\not{p}_T). In our present work, we use a fixed collider energy ($\sqrt{s} = 500$ GeV) for the mass measurement.

We first discuss the available mSUGRA parameter space in Sec. 2, followed by an analysis of the signals and cross sections in Sec. 3. Monte Carlo (MC) studies on the event selection cuts to probe the SUSY events and the SM background are reported in Sec. 4 and the precision in the mass measurements in Sec. 5. We conclude in Sec. 6.

2 mSUGRA Parameter Space

The models of mSUGRA depends on only four parameters and one sign. These are m_0 (the universal soft breaking mass at the GUT scale M_G); $m_{1/2}$ (the universal gaugino soft breaking mass at M_G); A_0 (the universal cubic soft breaking mass at M_G); $\tan\beta = \langle H_2 \rangle / \langle H_1 \rangle$ at the electroweak scale (where H_2 gives rise to u quark masses and H_1 to d quark and lepton masses); and the sign of μ , the Higgs mixing parameter in the superpotential ($W_\mu = \mu H_1 H_2$). Note that the lightest neutralino $\tilde{\chi}_1^0$ and the gluino \tilde{g} are approximately related to $m_{1/2}$ by $M_{\tilde{\chi}_1^0} \cong 0.4 m_{1/2}$ and $M_{\tilde{g}} \cong 2.8 m_{1/2}$.

The model parameters are already significantly constrained by different experimental results. Most important for limiting the parameter space are:

- The light Higgs mass bound of $M_{h^0} > 114$ GeV from LEP [8]. Since theoretical calculations of M_{h^0} still have a 2-3 GeV error, we will conservatively assume this to mean that $(M_{h^0})^{\text{theory}} > 111$ GeV.
- The $b \rightarrow s\gamma$ branching ratio [9]. We assume here a relatively broad range (since there are theoretical errors in extracting the branching ratio from the data):

$$1.8 \times 10^{-4} < \mathcal{B}(B \rightarrow X_s \gamma) < 4.5 \times 10^{-4} \quad (1)$$

- In mSUGRA the $\tilde{\chi}_1^0$ is the candidate for CDM. Previous bounds from balloon flights (Boomerang, Maxima, Dasi, etc.) gave a relic density bound for CDM of $0.07 < \Omega_{\text{CDM}} h^2 < 0.21$ (where Ω_{CDM} is the density of dark matter relative to the critical density to close the universe, and $h = H/100$ km/sec Mpc where H is the Hubble constant). However, the new data from WMAP [10] greatly tightens this (by a factor of four) and the 2σ bound is now:

$$0.095 < \Omega_{\text{CDM}} h^2 < 0.129 \quad (2)$$

- The bound on the lightest chargino mass of $M_{\tilde{\chi}_1^\pm} > 104$ GeV from LEP [11].
- The muon magnetic moment anomaly, δa_μ , using both μ^+ and μ^- data [12]. Using the e^+e^- data to calculate the SM leading order hadronic contribution, one gets a 2.7σ deviation of the SM from the experimental result [13, 14]. (The e^+e^- data appears to be more reliable than the τ decay data and Conserved Vector Current (CVC) analysis with CVC breaking [15].) Assuming the future data confirms the a_μ anomaly, the combined

effects of $g_\mu - 2$ and $M_{\tilde{\chi}_1^\pm} > 104$ GeV then only allow $\mu > 0$ and leave only the $\tilde{\tau}\text{-}\tilde{\chi}_1^0$ co-annihilation domain of the relic density.

One can now qualitatively state the constraints on the parameter space produced by the above experimental bounds: (a) The relic density constraint produces a narrow rising band of allowed parameter space in the $m_0\text{-}m_{1/2}$ plane; (b) In this band, the M_{h^0} and $b \rightarrow s\gamma$ constraints produce a lower bound on $m_{1/2}$ for all $\tan\beta$ of $m_{1/2} \gtrsim 300$ GeV, which implies $M_{\tilde{\chi}_1^0} > 120$ GeV and $M_{\tilde{\chi}_1^\pm} > 250$ GeV.

In the following, we will analyze the case of $\mu > 0$. In order to carry out the calculations it is necessary to include a number of corrections to obtain results of sufficient accuracy, and we list some of these here: (i) two loop gauge and one loop Yukawa renormalization group equations (RGEs) are used from M_G to the electroweak scale, and QCD RGE below the electroweak scale for the light quarks; (ii) two loop and pole mass corrections are included in the calculation of M_{h^0} ; (iii) One loop corrections to M_b and M_τ are included [16]; (iv) large $\tan\beta$ SUSY corrections to $b \rightarrow s\gamma$ are included [17]; (v) all $\tilde{\tau}_1\text{-}\tilde{\chi}_1^0$ co-annihilation channels are included in the relic density calculation [18]. We do not include Yukawa unification or proton decay constraints as these depend sensitively on post GUT physics, about which little is known.

Figure 1 illustrates the constraints on the mSUGRA parameter space for $\tan\beta = 10, 40$ and 50 with $A_0 = 0$. The narrow blue band is the region now allowed by WMAP (see Eq. 2). The dotted pink lines are for different Higgs masses, and the light blue region would be excluded if $\delta a_\mu > 11 \times 10^{-10}$. The three short solid lines indicate the $\tilde{\chi}_1^0\text{-}p$ cross section values. In the case of $\tan\beta = 40$ they represent (from left) 0.03×10^{-6} pb, 0.002×10^{-6} pb, 0.001×10^{-6} pb and in the case of $\tan\beta = 50$ they represent (from left) 0.05×10^{-6} pb, 0.004×10^{-6} pb, 0.002×10^{-6} pb. In the case of $\tan\beta = 10$ they represent (from left) 5×10^{-9} pb and 1×10^{-9} pb. It is important to note that the narrowness of the allowed dark matter band is not a fine tuning. The lower limit of the band comes from the rapid annihilation of neutralinos in the early universe due to co-annihilation effects as the light $\tilde{\tau}_1$ mass, $M_{\tilde{\tau}_1}$, approaches the neutralino mass as one lowers m_0 . Thus the lower edge of the band corresponds to the lower bound of Eq. 2, and the band is cut off sharply due to the Boltzman exponential behavior. The upper limit of the band, corresponding to the upper bound of Eq. 2, arises due to insufficient annihilation as m_0 is raised. As the WMAP data becomes more accurate, the allowed band will narrow even more. (Note that the slope and position of the band changes, however as A_0 is changed.) Thus the astronomical determination of the amount of dark matter effectively determines one combination of the four parameters of mSUGRA. Since the $\tilde{\tau}\text{-}\tilde{\chi}_1^0$ co-annihilation region seems to be experimentally most favored (including the $g - 2$ effect), we probe this region. Let us now study the available sparticles when we try to probe this co-annihilation band in a linear collider.

3 Production and Signals of SUSY Particles at an ILC

Figure 1 shows the production cross section of 0.1 fb for $\tilde{e}_R^+\tilde{e}_R^-$ (black dashed), $\tilde{\tau}_1^+\tilde{\tau}_1^-$ (blue solid), $\tilde{\chi}_1^0\tilde{\chi}_2^0$ (blue dashed-dot) and chargino pair (vertical black dot) productions. We see that for large $\tan\beta$ the chargino pair production is almost not observable and the selectron pair production is unobservable. The stau pair has the largest reach in $m_{1/2}$ and the neutralino

pair has the largest reach in m_0 . We therefore focus on the stau pair and the neutralino pair production cross sections. The kinematical reach of the production cross sections of $\tilde{\tau}_1^+ \tilde{\tau}_1^-$ and $\tilde{\chi}_1^0 \tilde{\chi}_2^0$ productions for both $\sqrt{s} = 500$ and 800 GeV are shown in the figures. We see that the 800 GeV ILC will have a much bigger reach. We will, however, use the 500 GeV collider to study the signal since it seems to be the initial CM energy for ILC.

The possible signals for $\tilde{\tau}_1^+ \tilde{\tau}_1^-$ and $\tilde{\chi}_1^0 \tilde{\chi}_2^0$ in mSUGRA are the following:

$$e^+ e^- \rightarrow \tilde{\tau}_1^+ \tilde{\tau}_1^- \rightarrow (\tau^+ \tilde{\chi}_1^0) + (\tau^- \tilde{\chi}_1^0) \quad (3)$$

$$e^+ e^- \rightarrow \tilde{\chi}_1^0 \tilde{\chi}_2^0 \rightarrow \tilde{\chi}_1^0 + (\tau \tilde{\tau}_1) \rightarrow \tilde{\chi}_1^0 + (\tau^+ \tau^- \tilde{\chi}_1^0) \quad (4)$$

We look at the hadronic final state of taus (τ_h 's) in order to have larger event rates. The final signal thus has two τ_h 's plus \cancel{p}_T . The analysis now is quite complicated since the τ 's have low energy due to a small ΔM value. We need to develop appropriate event selection cuts to extract the signal from the SM background which is dominated by the $\gamma^* \gamma^* e^+ e^-$.

In general, the co-annihilation region occurs for $\Delta M \sim 5$ -15 GeV. We choose three points for $m_{1/2} = 360$ GeV, $m_0 = 205, 210$ and 220 GeV, with $A_0 = 0$ and $\tan \beta = 40$ and develop our event selection cuts. The masses of SUSY particles in these three representative scenarios are given in Table 1. The values of ΔM for these three points are 5, 10 and 19 GeV. The first selection we use is the electron beam polarization. Since both signals and background processes cross sections are affected by it, we choose appropriate polarization to increase the significance of the signal. The production cross sections for $\sqrt{s} = 500$ GeV for different polarizations are given in Table 2. The right-handed (RH) polarization $\mathcal{P}(e^-) = -0.9$ enhances the $\tilde{\tau}_1^+ \tilde{\tau}_1^-$ signal, and the left-handed (LH) polarization, $\mathcal{P}(e^-) = +0.9$ enhances the $\tilde{\chi}_1^0 \tilde{\chi}_2^0$ signal. The SM background, mentioned in table, consists of $\bar{\nu} \nu \tau^+ \tau^-$ states arising from WW , ZZ and $Z\nu\nu$ production and this background becomes smaller for a right-handed electron beam. In addition to this, we also have two photon processes which will be described later: $e^+ e^- \rightarrow \gamma^* \gamma^* + e^+ e^- \rightarrow \tau^+ \tau^-$ (or $q\bar{q}$) + $e^+ e^-$ where the final state $e^+ e^-$ pair are at a small angle to the beam pipe and the $q\bar{q}$ jets fake a $\tau^+ \tau^-$ pair. This background, does not change with beam polarization and needs to be suppressed by appropriate cuts.

Table 1: Masses (in GeV) of SUSY particles in three representative scenarios of $\Delta M \equiv M_{\tilde{\tau}_1} - M_{\tilde{\chi}_1^0}$ for $m_{1/2} = 360$ GeV, $\tan \beta = 40$, $\mu > 0$, and $A_0 = 0$. These points satisfy all the existing experimental bounds on mSUGRA. The numbers were obtained using ISAJET [19].

MC Point (m_0 in GeV)	$M_{\tilde{\chi}_2^0}$	$M_{\tilde{\tau}_1}$	$M_{\tilde{\chi}_1^0}$	ΔM
1 (205)	274.2	147.2	142.5	4.76
2 (210)	274.2	152.0	142.5	9.53
3 (220)	274.3	161.6	142.6	19.0

The event selection cuts with the LH polarization will be optimized to enhance the $\tilde{\chi}_1^0 \tilde{\chi}_2^0$ signal and the RH cuts to optimize the $\tilde{\tau}_1^+ \tilde{\tau}_1^-$ signal.

Table 2: Cross section times branching ratio (in fb), $\sigma \times \mathcal{B}(\tau \rightarrow \tau_h)^2$, for SUSY and SM 4-fermions (4f) production in two cases of polarizations, $\mathcal{P}(e^-) = -0.9$ (RH) and $+0.9$ (LH). The SUSY cross sections were obtained using **ISAJET** [19], and **WPHACT** [20] was used for the cross sections of the $\bar{\nu}\nu\tau^+\tau^-$ processes.

$\mathcal{P}(e^-)$		-0.9 (RH)	0.9 (LH)
SM 4f		7.84	89.8
SUSY point 1	$\tilde{\chi}_1^0 \tilde{\chi}_2^0$	0.41	6.09
	$\tilde{\tau}_1^+ \tilde{\tau}_1^-$	28.3	13.2
SUSY point 2	$\tilde{\chi}_1^0 \tilde{\chi}_2^0$	0.40	6.00
	$\tilde{\tau}_1^+ \tilde{\tau}_1^-$	26.6	12.4
SUSY point 3	$\tilde{\chi}_1^0 \tilde{\chi}_2^0$	0.38	5.68
	$\tilde{\tau}_1^+ \tilde{\tau}_1^-$	23.0	10.6

The generation of MC samples and the analysis for the signal and the background was done using the following programs: (1) **ISAJET** [19] to generate SUSY events; (2) **WPHACT** [20] for SM backgrounds; (3) **TAUOLA** [21] for tau decay; (4) Events were simulated and analysed with a LC detector simulation [22].

3.1 Event Selection

In order to reduce the backgrounds we require a set of event selection cuts and these cuts are given in Table 3. In this table: j_2 stands for second leading τ jet, p_{vis} gives the sum of visible momenta and $\theta(j_2, p_{vis})$ is the angle between them. θ_{jet} is the angle between a τ jet and the beam direction. The jets are reconstructed using the JADE algorithm with $Y_{cut} \geq 0.0025$ [23] and selected with $E_{jet} > 3$ GeV. Such a value of the Y_{cut} parameter helps to select narrow τ -like jets. The jet acceptance cut is required to reduce the SM background events such as WW and ZZ production. The acoplanarity is defined as $\mathcal{A} = 180^\circ - \Delta\phi(j_1, j_2)$, where $\Delta\phi(j_1, j_2)$ is the azimuthal angle between two τ -jets. The cut on acoplanarity is very powerful in rejecting two photon SM backgrounds which have a huge cross section. In order to have MC samples of manageable size for two photon SM processes we apply a cut $\mathcal{A}_{MC} > 30^\circ$ already at the generator level. (In addition for these samples we apply the generator level cut on $p_T^{\tau MC} > 4$ GeV and require the τ to be separated from the beam line by more than 35°). We also require no EM clusters (a) in $5.8^\circ < \theta < 28^\circ$ where the ILC detector has no tracking system and (b) in the angle below 5.8° with two options of a very forward calorimeter (VFD). In our calculation, beamstrahlung and bremsstrahlung are included in the two-photon annihilation process. The two photon background in our analysis is similar to that discussed in Refs. [6, 7].

The number of accepted events for each class of final states for the case $p_T > 5$, 10, and 20 GeV are summarized in Table 4.

- The RH polarization strongly suppresses the SM background events (WW etc.) and the neutralino events ($\tilde{\chi}_1^0 \tilde{\chi}_2^0$). We also need a 1° VFD and $p_T > 5$ GeV to get a clean signal for

Table 3: Kinematic cuts for the LH ($\mathcal{P} = 0.9$) and the RH ($\mathcal{P} = -0.9$) cases

Cut Variable(s)	LH ($\mathcal{P}(e^-) = 0.9$)	RH ($\mathcal{P}(e^-) = -0.9$)
$N_{jet}(E_{jet} > 3 \text{ GeV})$	2	
τ_h ID	1, 3 tracks; $M_{tracks} < 1.8 \text{ GeV}$	
Jet acceptance	$-q_{jet} \cos \theta_{jet} < 0.7$ $-0.8 < \cos \theta(j_2, p_{vis}) < 0.7$	$ \cos \theta_{jet} < 0.65$ $ \cos \theta(j_2, p_{vis}) < 0.6$
Missing p_T	$> 5 \text{ GeV}$	
Acoplanarity	$> 40^\circ$	
Veto on EM clusters or electrons	No EM cluster in $5.8^\circ < \theta < 28^\circ$ with $E > 2 \text{ GeV}$ No electrons within $\theta > 28^\circ$ with $p_T > 1.5 \text{ GeV}$	
Very forward calorimeter ($1^\circ(2^\circ) - 5.8^\circ$)	No EM cluster with $E > 100 \text{ GeV}$	

the $\tilde{\tau}_1^+ \tilde{\tau}_1^-$ events. With no VFD there would be approximately 4,400 SM $\gamma\gamma$ background events swamping the SUSY signal.

- The LH polarization allows for the detection of the $\tilde{\chi}_1^0 \tilde{\chi}_2^0$ signal with $\not{p}_T > 20 \text{ GeV}$ without a VFD (as the $\gamma\gamma$ background falls to zero then), or $\not{p}_T > 10 \text{ GeV}$ with a 2° VFD. However, both a 1° VFD and $\not{p}_T > 5 \text{ GeV}$ are necessary to detect the $\tilde{\tau}_1^+ \tilde{\tau}_1^-$ events and to measure ΔM in the LH case. In the case of no VFD there would be $\sim 9,300$ SM $\gamma\gamma$ background events with $\not{p}_T > 5 \text{ GeV}$. Note that the event selection criteria in the LH polarization case are different from the RH case.

Thus we find that the VFD is essential to detect SUSY in this region of parameter space. A lower \not{p}_T increases the number of events and the significance. A 5 GeV \not{p}_T cut has been found to be feasible at a 500 GeV ILC.

It should be noted that the 1° VFD is feasible for the ILC since the TESLA design (which has been accepted for the ILC technology) allows a VFD coverage down to 3.2 mrad (or 0.18°) [1]. We also note that our study is based on head-on collisions of electron and positron. However, it has been shown that the VFD is still able to reduce the two-photon background events even in the case of a beam crossing [7].

The $\tilde{\tau}_1^+ \tilde{\tau}_1^-$ cross section has the largest reach along the co-annihilation band and one would use this channel to measure the mass difference. This channel needs RH polarization for enhancement. In Figure 2, we plot the number of events accepted in our selection criteria with 500 fb^{-1} of luminosity as a function of ΔM for $m_0 = 203\text{-}220 \text{ GeV}$ ($m_{1/2} = 360 \text{ GeV}$) in the RH polarization case. We see that we have more than 100 events, which will be adequate for the measurement of ΔM as discussed in Section 4, for $\Delta M > 4.5 \text{ GeV}$. Figure 3 is a plot of the acceptance as a function of ΔM for $m_0 = 203\text{-}220 \text{ GeV}$ with a 1° VFD in the case of RH polarization. The acceptance drops rapidly as ΔM goes below 5 GeV .

The event acceptance also depends on $m_{1/2}$ as shown in Figure 4. This dependence arises because the τ 's are less energetic and its angular distribution changes as the stau becomes

Table 4: Number of $\tau_h\tau_h$ plus \cancel{p}_T events for luminosity of 500 fb⁻¹ for points 1, 2 and 3 corresponding to $\Delta M = 4.76, 9.5$, and 19.0 GeV, respectively. All numbers except for two-photon backgrounds are common for different options of VFD.

Process		$\mathcal{P}(e^-) = 0.9$ (LH)			$\mathcal{P}(e^-) = -0.9$ (RH)		
		$\cancel{p}_T^{min} = 5$	10	20	5	10	20
$\tilde{\chi}_2^0\tilde{\chi}_1^0$	Pt.1	374	342	260	15	14	11
	Pt.2	624	572	425	26	24	18
	Pt.3	743	697	529	29	28	22
$\tilde{\tau}^+\tilde{\tau}^-$	Pt.1	73	2	0	122	2	0
	Pt.2	524	267	11	786	437	22
	Pt.3	946	781	335	1283	1076	468
SM 4f		1745	1626	1240	129	123	100
SM $\gamma\gamma$	2-5.8° VFD	535	7	0	249	4	0
	1-5.8° VFD	10	0	0	4	0	0

heavier. We calculate the significance (σ) as $N_{\text{signal}}/\sqrt{N_{\text{BG}}}$, where the $\tilde{\chi}_1^0\tilde{\chi}_2^0$ events are also treated as backgrounds, for a window of $M_{\text{eff}} \equiv M(j_1, j_2, \cancel{E})$ (invariant mass of two τ -jets and missing energy). For $\Delta M = 4.76$ and 19 GeV, the allowed ranges for M_{eff} are 0-54.5 GeV and 0-183.5 GeV, respectively. The 5σ reach for the $\tilde{\tau}_1$ mass is found to be ≤ 215 GeV ($m_{1/2} \leq 520$ GeV) for $\Delta M = 4.76$ GeV with a 1° VFD and $\cancel{p}_T > 5$ GeV. For $\Delta M = 19$ GeV, the 5σ reach of the $\tilde{\tau}$ mass at a 500 GeV ILC is ≤ 237 GeV ($m_{1/2} \leq 537$ GeV).

It should be noted that our event selection cuts are optimized for a 500 GeV machine. In the case of an 800 GeV ILC, the cuts need to be re-optimized based on the new SUSY backgrounds and machine design limitations (e.g. the lower bound on \cancel{p}_T needs to be raised).

4 Measurement of Stau Neutralino Mass Difference

The measurement of a small ΔM value is crucial since it would be a key evidence of the existence of the $\tilde{\tau}\tilde{\chi}_1^0$ co-annihilation. We propose the variable M_{eff} as a key discriminator of the signal events from its background events. We first generate the high statistics MC samples for the SM and various SUSY events (by changing the m_0 value) and prepare the templates of the M_{eff} distributions for the SM, $\tilde{\chi}_1^0\tilde{\chi}_2^0$, and $\tilde{\tau}_1^+\tilde{\tau}_1^-$ events. Figure 5 (without the data points for 500 fb⁻¹) shows examples of such templates for two m_0 values for a 2° VFD in the RH polarization case. The SM cross section is fitted by a blue line, the stau pair by a green line and the neutralino pair by a red line. The stau pair production peak separates from the SM background as ΔM increases. This is because for smaller ΔM , the two τ signal appears like the τ 's from the two photon background and consequently this region requires a VFD coverage down to 1°. From Figure 5 we also find that the stau pair production cross section can be measured upto an accuracy of $\pm 4\%$ for Point 2.

Since the data of 500 fb⁻¹ of luminosity will be generated in the initial run for a few years,

Table 5: Accuracy of the determination of ΔM for different VFDs.

m_0	ΔM	$N_{\tilde{\tau}_1^+ \tilde{\tau}_1^-}$ (500 fb $^{-1}$)	ΔM (“500 fb $^{-1}$ ” experiment)	
			2° VFD	1° VFD
205	4.76	122	Not Determined	$4.7_{-1.0}^{+1.0}$
210	9.53	787	$9.5_{-1.0}^{+1.1}$	$9.5_{-1.0}^{+1.0}$
213	12.4	1027	$12.5_{-1.4}^{+1.4}$	$12.5_{-1.4}^{+1.1}$
215	14.3	1138	$14.5_{-1.4}^{+1.1}$	$14.5_{-1.4}^{+1.1}$

we then generate the MC samples equivalent to 500 fb $^{-1}$ of luminosity for particular ΔM values and fit them with the template functions generated for high statistics sample. The black lines in Figure 5 shows the fitting of the 500 fb $^{-1}$ MC samples for point 2 with the templates of two different m_0 values of 210 and 211 GeV. (Other parameters are kept at the same values as before.) We then compare the χ^2 for these fits. We find that the χ^2 for these fits is minimum for the $m_0 = 210$ GeV case. We use the range of $m_0 = 203$ -220 GeV and try to fit the 500 fb $^{-1}$ MC sample for point 2 and determine the χ^2 for all these different points. We plot the χ^2 of these fits in Figure 6 and find that 1σ in the χ^2 corresponds to 9.5 ± 1 GeV. The true value of ΔM for the point 2 is 9.53 GeV. We repeat the same study for different $\tilde{\tau}_1$ masses i.e. for different ΔM . For lower ΔM (~ 5 GeV), we need to use a VFD of 1°. The accuracy of mass determination for two different VFDs is summarized in Table 5, showing the uncertainties are at a level of 10%, except for $\Delta M \sim 5$ GeV where it is 20% and we have 100 $\tilde{\tau}_1^+ \tilde{\tau}_1^-$ events.

Figure 7 illustrates the $\tilde{\tau}_1$ mass reach as a function of luminosity for a 5σ discovery with at least 100 events for $\Delta M \sim 5$ GeV, where the ΔM would be determined to 20% or better. We find that 164 GeV and 205 GeV $\tilde{\tau}_1$ masses to be 5σ reach and 20% (or better) uncertainty in ΔM measurement with 500 and 2500 fb $^{-1}$ at a 500 GeV ILC.

5 Conclusion

We have probed the mSUGRA and SM signals in the $\tilde{\tau}-\tilde{\chi}_1^0$ co-annihilation region at a 500 GeV ILC with 500 fb $^{-1}$ of luminosity. In this region, the mass difference ΔM between the $\tilde{\tau}_1$ and the $\tilde{\chi}_1^0$ would typically be 5-15 GeV for a large range of $m_{1/2}$. This small mass difference would produce very low energy taus in the final state. The dominant SM background would be the two-photon process. With RH e^- beams our study has focused on the $\tilde{\tau}^+ \tilde{\tau}^-$ production because it allowed us to reach large $m_{1/2}$ values in the allowed parameter space. We proposed the invariant mass of two tau jets and missing energy variable, $M(j_1, j_2, \cancel{E})$, to determine the mass difference and found the accuracy would be at a level of 10% using a 1° (or 2°) VFD except for $\Delta M = 4.76$ GeV. For $\Delta M \simeq 5$ GeV, a 1° VFD would be crucial to suppress the two-photon background and the accuracy there would be about 20% with approximately 100 signal events. We also calculated the discovery significance of this region and determined the 5σ reach in $m_{1/2}$ for 500 fb $^{-1}$ of luminosity.

6 Acknowledgments

This work is supported in part by a NSF Grant PHY-0101015, in part by NSERC of Canada and in part by a DOE Grant DE-FG02-95ER40917.

References

- [1] TESLA: Technical design report, part 4: A detector for TESLA, T. Behnke *et al.*, DESY-2001-011, DESY-2001-011D, DESY-TESLA-2001-23, DESY-TESLA-FEL-2001-05, ECFA-2001-209, March 2001. In a recent upgrade of the final focus setup, the forward calorimeter, low angle tagger or LAT, covers an angle down to 3.2 mrad.
- [2] A.H. Chamseddine, R. Arnowitt, and P. Nath, Phys. Rev. Lett. **49** (1982) 970.
- [3] R. Barbieri, S. Ferrara, and C. A. Savoy, Phys. Lett. **B119** (1982) 343; L. Hall, J. Lykken, and S. Weinberg, Phys. Rev. **D27** (1983) 2359; P. Nath, R. Arnowitt, and A.H. Chamseddine, Nucl. Phys. **B227** (1983) 121.
- [4] For a review, P. Nilles, Phys. Rept. **110** (1984) 1.
- [5] J. Ellis, K. Olive, Y. Santoso, and V. Spanos, Phys. Lett. **B565** (2003) 176; R. Arnowitt, B. Dutta, T. Kamon, and V. Khotilovich, hep-ph/0308159; H. Baer, C. Balazs, A. Belyaev, T. Krupovnickas, and X. Tata, JHEP **0306** (2003) 054; B. Lahanas and D.V. Nanopoulos, Phys. Lett. **B568** (2003) 55; U. Chattopadhyay, A. Corsetti, and P. Nath, Phys. Rev. **D68** (2003) 035005.
- [6] H. Baer, T. Krupovnickas, and X. Tata, JHEP **0406** (2004) 061.
- [7] P. Bambade, M. Berggren, F. Richard, and Z. Zhang, hep-ph/0406010.
- [8] See, for example, P. Igo-Kemenes, LEPC meeting, (<http://lephiggs.web.cern.ch/LEPHIGGS/talks/index.html>).
- [9] M. Alam *et al.*, Phys. Rev. Lett. **74** (1995) 2885.
- [10] WMAP Collaboration, D.N Spergel *et al.*, Astrophys. J. Suppl. **148** (2003) 175.
- [11] ALEPH collaboration, ALEPH-CONF-2001-009.
- [12] Muon $g - 2$ Collaboration, G. Bennett *et al.*, Phys. Rev. Lett. **92** (2004) 161802.
- [13] M. Davier, hep-ex/0312065.
- [14] K. Hagiwara, A. Martin, D. Nomura, and T. Teubner, Phys. Rev. **D69** (2004) 093003.
- [15] W. Marciano, hep-ph/0411179.
- [16] R. Rattazi and U. Sarid, Phys. Rev. **53** (1996) 1553; M. Carena, M. Olechowski, S. Pokorski, and C. Wagner, Nucl. Phys. **426** (1994) 269.
- [17] G. Degrandi, P. Gambino, and G. Giudice, JHEP **0012** (2000) 009; M. Carena, D. Garcia, U. Nierste, and C. Wagner, Phys. Lett. **B499** (2001) 141; G. D'Ambrosio, G. Giudice, G. Isidori, and A. Strumia, hep-ph/0207036; A. Buras, P. Chankowski, J. Rosiek, and L. Slawianowska, hep-ph/0210145.

- [18] R. Arnowitt, B. Dutta, and Y. Santoso, hep-ph/0010244; hep-ph/0101020; Nucl. Phys. **B606** (2001) 59; J. Ellis, T. Falk, G. Gani, K. Olive, and M. Srednicki, Phys. Lett. **B570** (2001) 236; J. Ellis, T. Falk, and K. Olive, Phys. Lett. **B444** (1998) 367; J. Ellis, T. Falk, K. Olive, and M. Srednicki, Astro. Phys. **13** (2000) 181; Erratum-ibid. **15** 2001 413; M. Gomez, and J. Vergados, Phys. Lett. **B512** (2001) 252; M. Gomez, G. Lazarides, and C. Pallis, Phys. Rev. **D61** (2000) 123512; Phys. Lett. **B487** (2000) 313; L. Roszkowski, R. Austri, and T. Nihei, JHEP **0108** (2001) 024; A. Lahanas, D.V. Nanopoulos, and V. Spanos, Phys. Lett. **B518** (2001) 518.
- [19] F. Paige, S. Protopescu, H. Baer, and X. Tata, hep-ph/0312045. We use ISAJET version 7.69.
- [20] E. Accomando and A. Ballestrero, Comput. Phys. Commun. **99** (1997) 270; E. Accomando, A. Ballestrero, and E. Maina, Comput. Phys. Commun. **150** (2003) 166. We use WPHACT version 2.02pol.
- [21] S. Jadach and J. H. Kühn, Comput. Phys. Comm. **64** (1991) 275; M. Jezabek, Z. Was, S. Jadach, and J. H. Kühn, Comput. Phys. Comm. **70** (1992) 69; M. Jezabek, Z. Was, S. Jadach, and J. H. Kühn, Comput. Phys. Comm. **76** (1993) 361. We use TAUOLA version 2.6.
- [22] LCD Root Package version 3.5 with LD Mar01 detector parametrization. See, for example, T. Abe and M. Iwasaki, in Proc. of the APS/DPF/DPB Summer Study on the Future of Particle Physics (Snowmass 2001), ed. N. Graf, eConf **C010630**, E3045 (2001) [hep-ex/0110068].
- [23] JADE collaboration, W. Bartl *et al.*, Z. Phys **C33** (1986) 23; S. Bethke *et al.*, Phys. Lett. **B213** (1988) 235.

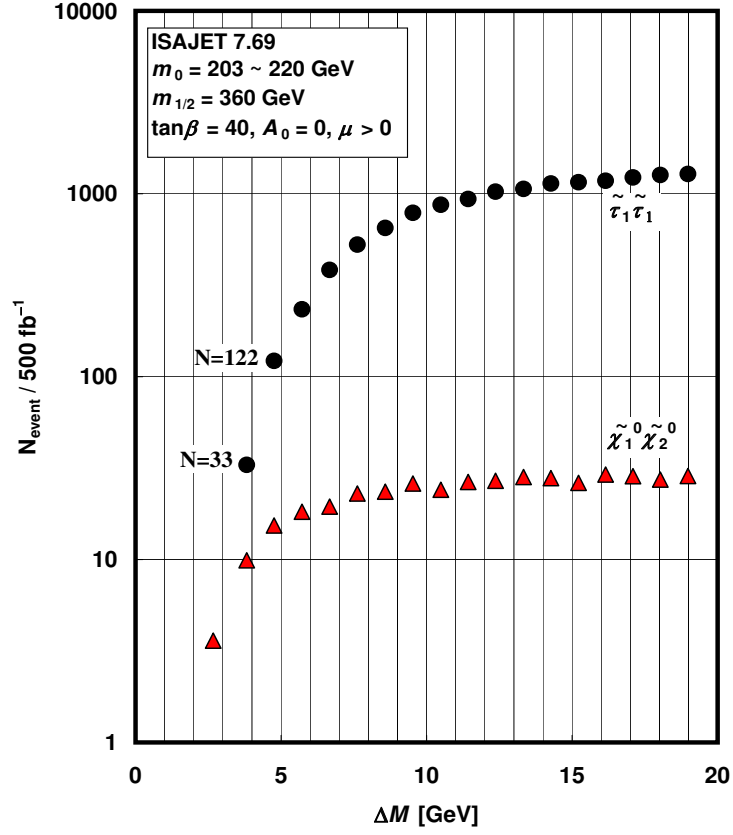


Figure 2: Number of $\tau_h \tau_h \tilde{\chi}_1^0 \tilde{\chi}_1^0$ events from $\tilde{\tau}_1^+ \tilde{\tau}_1^-$ (solid circles) and $\tilde{\chi}_1^0 \tilde{\chi}_2^0$ (solid triangles) production as a function of ΔM (for $m_0 = 203\text{--}220$ GeV at $m_{1/2} = 360$ GeV) in the RH polarization case. We assume 500 fb^{-1} of luminosity.

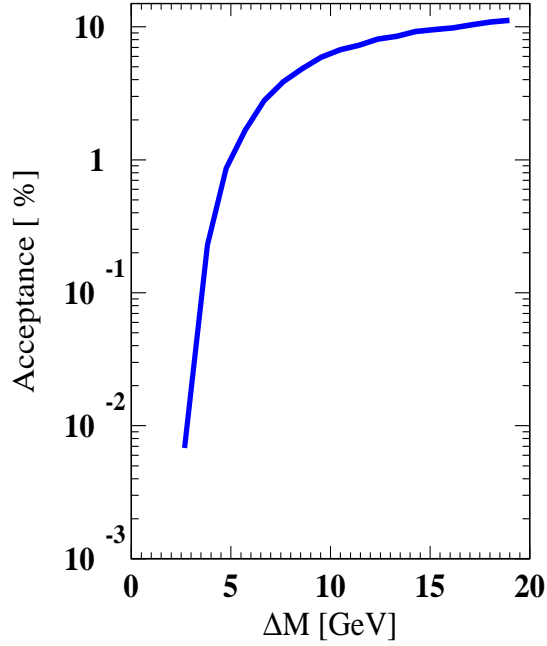


Figure 3: Total event acceptance for $\tilde{\tau}_1^+ \tilde{\tau}_1^- \rightarrow \tau_h \tau_h \tilde{\chi}_1^0 \tilde{\chi}_1^0$ as a function of ΔM for $m_0 = 203\text{--}220$ GeV ($m_{1/2} = 360$ GeV) in the RH polarization case.

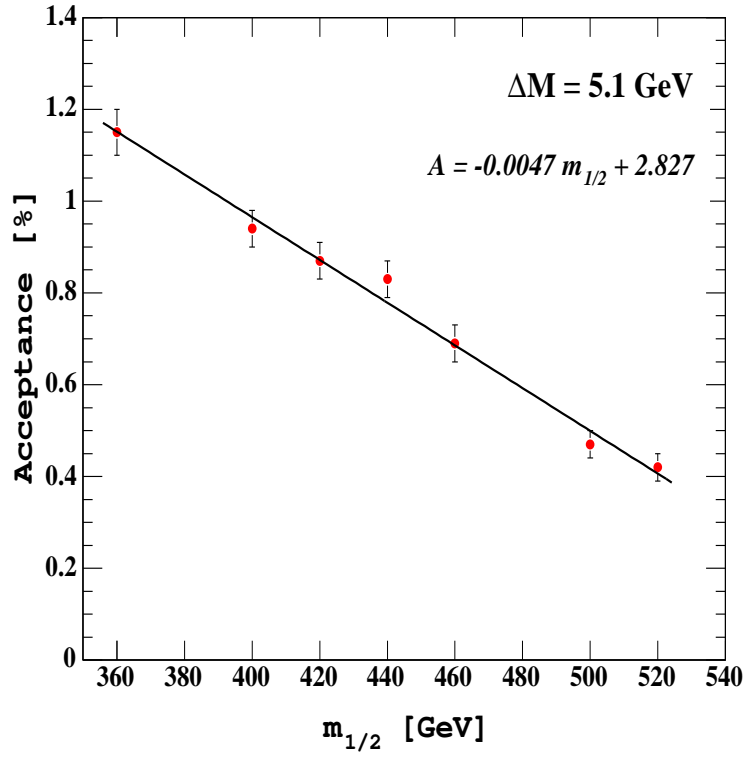


Figure 4: Total event acceptance for $\tilde{\tau}_1^+ \tilde{\tau}_1^- \rightarrow \tau_h \tau_h \tilde{\chi}_1^0 \tilde{\chi}_1^0$ as a function of $m_{1/2}$ for $\Delta M = 5.1$ GeV in the RH polarization case.

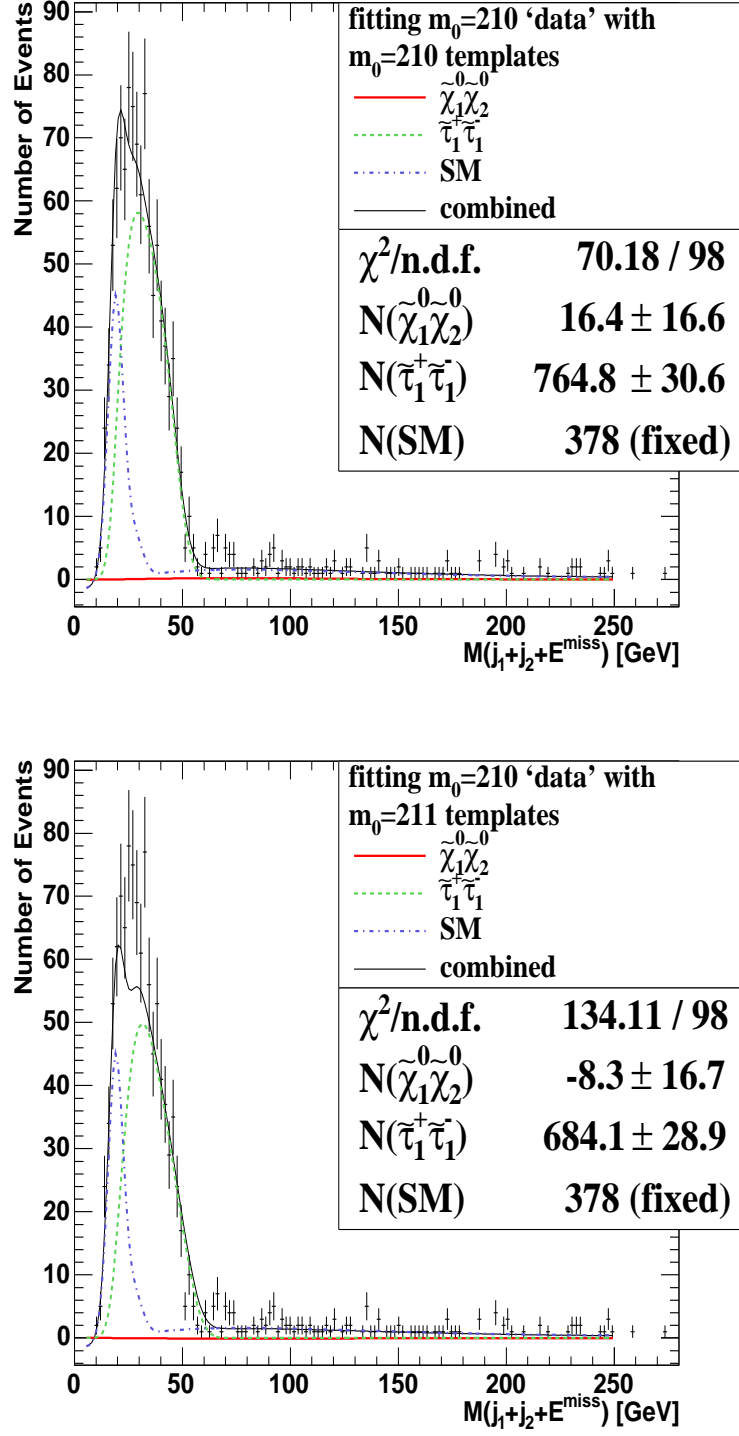


Figure 5: Example of fitting a MC sample containing SM and SUSY ($m_0 = 210$ GeV, $m_{1/2} = 360$ GeV) events equivalent to 500 fb^{-1} to two M_{eff} templates for SM+SUSY ($m_0 = 210$ or 211 GeV, $m_{1/2} = 360$ GeV). A 2° VFD is assumed. The value of $\chi^2/\text{n.d.f.}$ is minimum when the events from the same SUSY parameter are in the 500 fb^{-1} sample. A $\gamma\gamma$ contribution (a narrow distribution around 20 GeV) is apparent. The fitting is similar for 1° VFD, except the $\gamma\gamma$ contribution is substantially reduced.

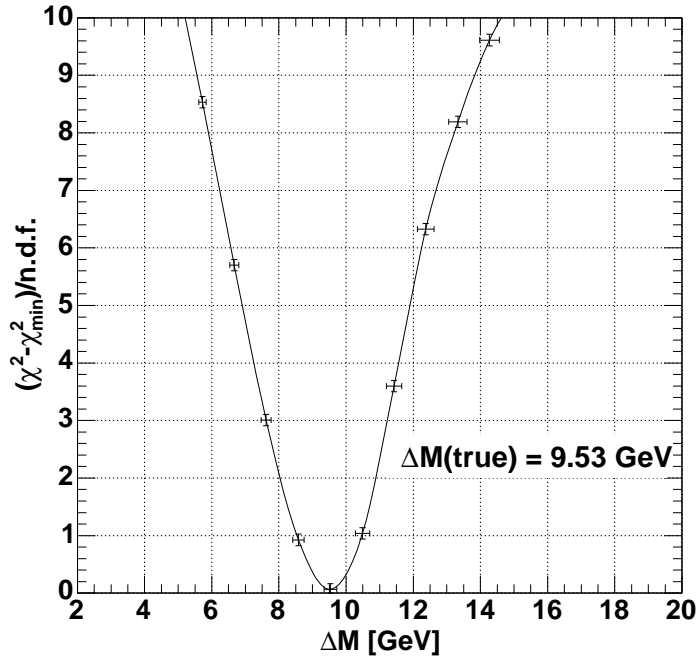


Figure 6: $\chi^2 - \chi^2_{\min}$ of fitting the 500 fb⁻¹ sample for SUSY Point 2 ($m_0 = 210$ GeV, $m_{1/2} = 360$ GeV) with the high statistics templates is plotted as a function of ΔM .

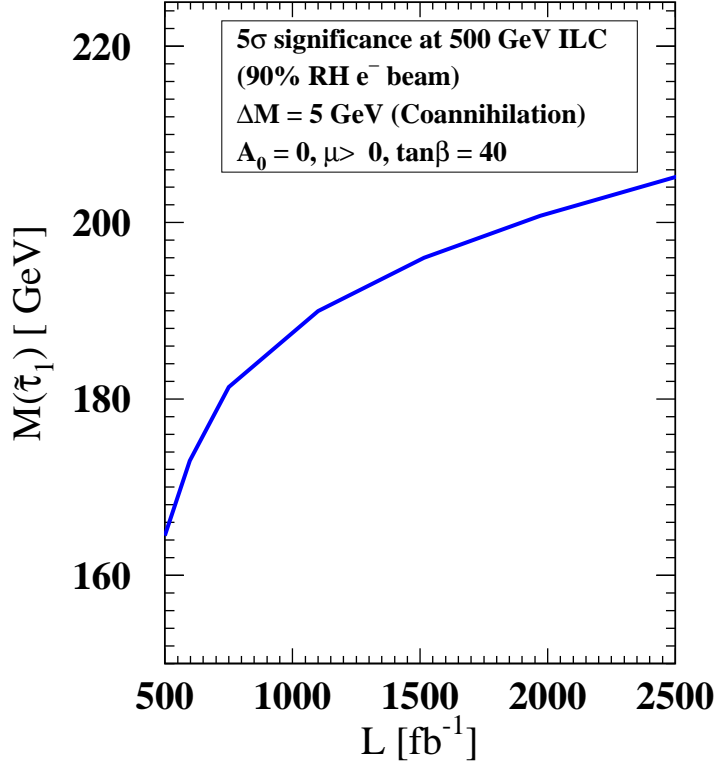


Figure 7: The $\tilde{\tau}_1$ mass reach with $\Delta M = 5$ GeV as a function of luminosity for a 5σ discovery with at least 100 events.